

INVITED REVIEW

# Laboratory studies of droplets in turbulence: towards understanding the formation of clouds

To cite this article: Z Warhaft 2009 *Fluid Dyn. Res.* **41** 011201

View the [article online](#) for updates and enhancements.

## Related content

- [DNS results of turbulent geometric collision rate](#)  
Orlando Ayala, Bogdan Rosa, Lian-Ping Wang et al.
- [Statistical models for predicting pair dispersion and particle clustering in isotropic turbulence and their applications](#)  
Leonid I Zaichik and Vladimir M Alipchenkov
- [Spatial clustering of polydisperse inertial particles in turbulence: II. Comparing simulation with experiment](#)  
Ewe-Wei Saw, Raymond A Shaw, Juan P L C Salazar et al.

## Recent citations

- [Time resolved measurements of droplet preferential concentration in homogeneous isotropic turbulence without mean flow](#)  
H. Lian *et al*
- [Fractal dimensions and trajectory crossings in correlated random walks](#)  
A. Dubey *et al*
- [A turbulent quarter century of active grids: from Makita \(1991\) to the present](#)  
Laurent Mydlarski

## INVITED REVIEW

# Laboratory studies of droplets in turbulence: towards understanding the formation of clouds

**Z Warhaft**

Sibley School of Mechanical and Aerospace Engineering, Cornell University and International Collaboration for Turbulence Research, Ithaca, NY 14853, USA

E-mail: [zw16@cornell.edu](mailto:zw16@cornell.edu)

Received 11 October 2007, in final form 11 April 2008

Published 18 December 2008

Online at [stacks.iop.org/FDR/41/011201](http://stacks.iop.org/FDR/41/011201)

Communicated by S Kida

**Abstract**

Recent developments in the study of droplet motion in turbulent flows are reviewed with emphasis on particle acceleration and clustering, and the effects of turbulence on raindrop formation. There is also some discussion of the relationship between laboratory experiments and field observations, of the history of laboratory experiments, and of the relationship between art and science in early cloud studies.

**1. Introduction**

The main purpose of this paper is to review recent advances in laboratory experiments that are aiding our understanding of the effects of turbulence on raindrop formation in clouds. There are some secondary objectives. Because of the complex interplay between the various mechanisms in clouds, their investigation requires both laboratory and field experiments. As in other areas of geophysics this sometimes causes problems in interpretation. The abstract nature of laboratory experiments, where a single aspect of the cloud is studied may be difficult to reconcile with field experiments, where all of the cloud mechanisms may be simultaneously at play. Thus I will discuss the dichotomy between laboratory and field experiments in terms of the history of cloud studies. Finally, apart from their scientific interest, clouds are visually exciting objects. They captivate the artist as well as the scientist, and at times there have been interactions between the two groups. I will allude to some of the influences between the artists and scientists.

Clouds are immensely complicated dynamical structures. They vary in shape, size and altitude. They generally involve the three phases of water, in states far from equilibrium, and they are in turbulent motion, driven by buoyancy and sometimes shear. There are large temperature changes due to condensation. Their fluid dynamical scales vary by as much as seven orders of magnitude, from millimeters to tens of kilometers and the droplets



**Figure 1.** Study of cumulus clouds, 1822 (oil on paper laid down on panel) by John Constable (1776–1837). Note the heterogeneity. Analysis of the cloud cover in European paintings show 70–75% cover in Constable’s time compared with 55–70% in the 20th century (Lamb, 1995). Such surveys, when correlated with temperature data provide information on climate change. Source: Yale Center for British Art, Paul Mellon Collection, USA/ The Bridgeman Art Library.



**Figure 2.** A developing cumulus cloud. Note the similarity of the cloud row to that of the Constable in figure 1. Photo, author.

evolve from condensation nuclei in the submicron range to raindrops of tens of millimeters diameter. Clouds are heterogeneous and entrainment effects are pronounced. There are often radiative and electrical effects. Following the early 19th century classification by Luke Howard of three basic cloud types (cirrus, cumulous and stratus), there are ten genera in current use. These are combinations such as alto cumulous, cirrostratus, altostratus and so on. Although the classification is somewhat arbitrary it attests to the large variation of cloud types. Their altitudes vary from greater than 6 km (a typical base height for cirrus clouds) to low lying stratus near ground level, although the storm bearing cumulonimbus stretch through the full vertical range. Casual observations testify not only to the heterogeneity of any one cloud, and of clusters of clouds of the same type, but also to the variation of cloud types at a given moment spread across the sky. This is captured in the painting of Constable (figure 1).

It will be useful, for the purpose of this review, to have in mind a ‘typical’ cloud. We will assume it is a cumulous cloud (figure 2). Consider its timescale, the time it takes to evolve from one characteristic shape to another. This is determined by the large-scale convective turbulence inside the cloud. A typical cumulous cloud has dimensions of a few kilometers

(in the vertical as well as the horizontal directions). The length scale of the largest eddies may be of the order of some hundreds of meters. The characteristic vertical convective velocity is of the order of meters per second. Following Shaw (2003), we will fix the characteristics of the turbulence in our cloud to be of length scale 100 m and velocity scale,  $1 \text{ m s}^{-1}$ . Thus the timescale is of the order of 100 s. This is consistent with our incidental observations which tell us the timescale is of the order of minutes; certainly not seconds, or hours. It is an inconvenient scale. Few of us can stay staring up for long enough to track and remember the whole cloud evolution, yet it is too short for the artist to easily capture. The motion of fire or of water waves fix our attention because of their rapid changes, whereas the dynamics of geological formations and galaxies are slow and provide the comfort of permanent structures. Clouds are at an intermediate scale, not quite ephemeral, certainly not permanent. This, combined with the interplay of the vast multiplicity of scales, causes great difficulties in our observations, and in our laboratory experiments.

This paper is by no means exhaustive, even on the matter of the laboratory experiments; it pertains mainly to work the author has had some involvement with. For a comprehensive discussion of particle–turbulence interactions in clouds, the reader is referred to the excellent review by Shaw (2003) and for a broad perspective on the physics of clouds, see Rogers and Yau (1989) and Pruppacher and Klett (1997). Experiments, theory and numerical simulations generally progress as a whole, one approach deriving inspiration from the other. Much of the motivation for the work described here comes from theory and simulations. The reader is referred to Shaw for a list of references up to 2003 and to the earlier review of Vaillancort and Yau (2000). More recent work on theory and simulations of relevance to the experiments are Cristini *et al* (2003), Collins and Keswani (2004), Falkovich and Pumir (2004), Kostinski and Shaw (2005), Chun *et al* (2005, Chen *et al* 2006) Cencini *et al* (2006), Kerstein and Krueger (2006), Yoshimoto and Goto (2007), Franklin *et al* (2005), Pinsky and Khain (2004) and Reimer *et al* (2007).

The outline of the paper is as follows. In section 2, some historical background is provided and the relation of the laboratory experiment to the complex reality is discussed. In section 3, some fundamentals of turbulence are reviewed in the context of experiments. Section 4 looks at recent developments in our ‘visualization’ of particles in turbulence by particle tracking techniques. In section 5, the relation of turbulence to raindrop formation is discussed and this is related to experiments and computations of inertial particles.

## 2. Some historical background

Many would argue that the scientific study of clouds began with the Luke Howard classification of 1803. For a detailed description of his work, as well as the earlier history of cloud observing and classification, the reader is referred to Hamblyn (2001). Throughout the 19th century, there was much interest in observing nature and the boundary between the arts and sciences, particularly with regard to the natural sciences including meteorology, was much less rigid than it is today. For example, the great German poet, Goethe was very much involved with science. He is well known for his studies of color and vision, but he also took a particular interest in the scientific classification of clouds. The most original sea-and-sky scape painter of the 19th century, J W M Turner, annotated his copy of Goethe’s ‘Theory of Colors’, and referred to it directly in the title of one of his paintings<sup>1</sup>. Keats, Byron and Shelley and many other of the Romantic writers were greatly affected by nature and mixed regularly with

<sup>1</sup> Light and color (Goethe’s theory)—The Morning After the Deluge—Moses writing the book of Genesis (The Tate Gallery, London).



**Figure 3.** Landscape with a rainbow by Joseph Mallord William Turner (1775–1851). Turner was preoccupied with the interaction of light with clouds. Here, as in many other of his paintings there is also a focus on abrupt frontal phenomena. Source: Phillips, The International Fine Art Auctioneers, UK/Photo Bonhams, London, UK/The Bridgeman Art Library.

the prominent scientists of the day. The chemist Humphry Davy, who was the president of the Royal Society and was actively engaged in the arts, was an acquaintance of Turner ([Hamilton 1998](#)). Perhaps the finest of all cloud painters, John Constable, who was aware of the work of Luke Howard, did detailed cloud studies in the 1820s over Hampstead Heath (figure 1). His work shows the patience and rigor of the scientific observer. He documented the weather patterns and stated ‘Painting is a science and should be pursued as an inquiry into the laws of nature’ ([Shields 2004](#)). J W M Turner strapped himself to the mast of a ship in a storm so he could better observe the turbulence of the skies and water around him. Like Constable he ‘never tired of going to Hampstead and would spend hours on the Heath studying the effects of atmosphere . . .’ ([Hamilton 1998](#)). While Constable (and Ruisdael, the great cloud painter of the 17th century) are famous for their cumulous clouds, Turner infused a dramatic quality into his paintings of stratus clouds and their interaction with light (figure 3). Aside from his artistic achievements, his paintings have been used to provide proxy information on aerosol depth in the atmosphere ([Zerefos \*et al\* 2007](#)).

It was the holistic approach to nature that affected science in the latter part of the 19th century, particularly in England, and it has singular relevance to the laboratory studies of clouds. The engineer, John Aitkin attempted to produce whole cyclones and glaciers in his laboratory bench-top experiments (see [Aitken 1923](#)). His objective was to capture all of nature in his experiments, not to isolate a particular phenomenon as we do when we do laboratory experiments today. In his analysis of the history of particle detectors, Galison ([1997](#)) argues that in the late 19th century experiments were evolving in two distinct directions; those of abstract science which were reductionist, and the morphological or the natural history approach. In the former, particular questions arising from observations of nature were posed and these questions suggested experiment that could address a particular phenomenon. A familiar contemporary example would be experiments of the dynamics of density stratified fluids in wind tunnels, where issues of rotation and topography are not included. In the morphological approach, the attempt is to include everything, to create nature in the laboratory. There is the tacit understanding that everything is interconnected and that by isolating one phenomenon there is a danger of dealing with something that is artificial and has nothing to do with nature itself. We tend to be imbued with the abstract approach but the dissonance between the two approaches still permeates science today.



**Figure 4.** Ben Nevis, where C T R Wilson observed clouds and other meteorological phenomena. Reproduced by permission of the Royal Meteorological Society.

The clash of the abstract and what Galison calls the mimetic approach is highlighted in the work of C T R Wilson, the discoverer of the cloud chamber that bears his name. As we will see, his work has continued to influence the present day investigation of clouds. In contrast with Aitkin, C T R Wilson had a strong background in science having studied biology, physics and chemistry at Manchester and Cambridge (Wilson 1965). He also had a deep love of nature and would explore the Scottish countryside as a student. His work in the laboratory on condensation nuclei, non equilibrium systems and thermodynamics was infused with his intense interest in meteorological phenomena. In the early 1890s, Wilson paid visits to the meteorological observatory at the top of Ben Nevis (figure 4), the highest mountain in Britain (Wilson 1954). There he observed the complex manifestations of mist, cloud and the associated optical phenomena, morning glories and lunar coronas, through the fog.

Like Aitkin, Wilson wished to mimic these in the laboratory (Galison 1997). He conducted laboratory experiments on expanding dust free air in a chamber and exposing it to electric fields. Wilson observed the formation of cloud nuclei and studied the condensation by systematically changing the expansion ratios. (Aitkin, who was more the realist seeded his air with dust particles. We know today, that it is small dust and salt particles that are primarily responsible for the nucleation of droplets in clouds.) Later, Wilson passed the newly discovered x-rays through his chamber and also observed nucleation. All of this work was motivated by the desire to understand clouds. But in 1911 by using photography, he was able to observe the tracks of charged particles (Wilson 1911). This was the turning point and the cloud chamber as we know it today, was born. His experiments changed from mimetic to abstract and the foundations of modern physics rest on these and subsequent experiments. Wilson's motivation is virtually forgotten by physicists but the dichotomy between abstract and mimetic science remain close to the surface. We will return to particle detectors in section 4 after providing some background on turbulence.

### 3. Some characteristics of turbulence and its relation to clouds

Most of our understanding of turbulence comes from placing a sensor, such as a hot wire anemometer, in a flow and measuring at a fixed point, or a number of points, as the fluid

passes by. This is known as the Eulerian approach. The sensor produces a time series that is a component of the velocity vector. If the flow is statistically stationary, temporal quantities can be converted into spatial ones by means of Taylor's frozen flow hypothesis (Tennekes and Lumley 1972). Or, as is often necessary in taking data in a cloud, an aircraft flies through the turbulence at constant speed. If the cloud is homogeneous it may be possible to convert temporal to spatial data. Using these methods, we have amassed a large amount of statistical data in various flows. The measurements of velocity structure functions and spectra have allowed us to verify the Kolmogorov prediction of their form (Kolmogorov 1941, Frisch 1995) and most current modeling and theory relies on data obtained using the Eulerian approach. However, these measurements do not directly yield information on the acceleration field,  $a(\mathbf{x}, t)$ , which is the sum of the temporal and spatial variation of velocity:

$$a_j(\mathbf{x}, t) = \frac{\partial u_j}{\partial t} + u_i \frac{\partial u_j}{\partial x_i}, \quad (1)$$

where  $u_j$  is the  $j$ th component of the fluid velocity and the usual summation over repeated indices is applied ( $i = 1, 2, 3$ ). By following the motion of a fluid particle, the so-called Lagrangian approach,  $a_j(\mathbf{x}, t)$  can be directly measured thereby providing deeper insight into the turbulence structure and dynamics. Tracking a particle is much more visual than the Eulerian measurement, enabling us to see the history of the particle motion. The Lagrangian approach also yields direct information on how particle pairs separate (Bourgoin *et al* 2006), which is necessary in building models of turbulent diffusion and mixing. While the importance of doing Lagrangian measurements has long been recognized (Richardson 1926), until recently there have been formidable challenges in doing quantitative measurements at realistic Reynolds numbers. As we will show, changes in particle velocity and acceleration take place extremely rapidly in turbulent flows.

We characterize the turbulence by the Taylor scale Reynolds number

$$R_\lambda \equiv \langle u^2 \rangle^{1/2} \lambda / \nu, \quad (2)$$

where  $\langle u^2 \rangle^{1/2}$  is the rms longitudinal velocity,  $\lambda$  is the Taylor microscale defined by  $\langle u^2 \rangle = \lambda^2 \langle (\partial u / \partial x)^2 \rangle$ ,  $\nu$  is the kinematic viscosity ( $1.5 \times 10^{-5} \text{ m}^2 \text{ s}^{-1}$  for air) and the angle brackets denote averaging. The best model we have to explain the multiscale nature of turbulence is the Richardson–Kolmogorov cascade (Tennekes and Lumley 1972) which assumes that energy is passed from the largest to the smallest scales without dissipation. Thus, the energy input rate at the largest scales is equal to the energy dissipation rate,  $\varepsilon$ , at the smallest scales and we can write

$$\varepsilon \sim \langle u^2 \rangle / \tau \sim \langle u^2 \rangle^{3/2} / \ell, \quad (3)$$

where  $\langle u^2 \rangle$ , the velocity variance of the longitudinal component is proportional to the kinetic energy of the turbulence and  $\tau$  is the characteristic timescale of the turbulence ( $\sim \ell / \langle u^2 \rangle^{1/2}$ , where  $\ell$  is the length scale of the energy containing eddies). The timescale  $\tau$  is the ‘memory’ of the turbulence structure. In one timescale, the memory of the large scale is lost. For turbulence that is isotropic at the small scales  $\varepsilon$  can also be determined from the longitudinal velocity derivative (Tennekes and Lumley 1972)

$$\varepsilon = 15\nu \langle (\partial u / \partial x)^2 \rangle. \quad (4)$$

From (2), (3) and (4) it follows that

$$R_\lambda \sim \varepsilon^{1/6} \ell^{2/3} / \nu^{1/2}. \quad (5)$$



For our idealized cumulous cloud,  $\ell = 100 \text{ m}$ ,  $\langle u^2 \rangle^{1/2} = 1 \text{ m s}^{-1}$  and  $\tau \sim 100 \text{ s}$  (see section 1). From (3) and (5), we find  $\varepsilon = 10^{-2} \text{ m}^2 \text{ s}^{-3}$  and  $R_\lambda \sim 3 \times 10^3$ . The total energy dissipated by the cloud is of the order of  $\ell^3 \rho \varepsilon = 10 \text{ kW}$  (we have taken  $\rho \sim 1 \text{ kg m}^{-3}$ ). Finally, we can determine the smallest length, time and velocity scales of the turbulence,  $\eta$ ,  $\tau_\eta$  and  $v_\eta$ , when viscous effects become significant at the end of the cascade (Tennekes and Lumley 1972),

$$\eta \equiv (v^3/\varepsilon)^{1/4}; \quad \tau_\eta \equiv (v/\varepsilon)^{1/2}; \quad v_\eta \equiv (v\varepsilon)^{1/4}. \quad (6)$$

For our cloud,  $\eta = 0.8 \text{ mm}$ ,  $\tau_\eta = 0.04 \text{ s}$  and  $v_\eta = 2.0 \times 10^{-2} \text{ m s}^{-1}$ . Notice that  $\ell/\eta = 1.3 \times 10^5$  confirming the large separation of scales alluded to in the introduction.

We can also determine the acceleration variance of the turbulence. Since the most rapid changes of velocity occur at the smallest scales, Kolmogorov scaling (Heisenberg 1948, Yaglom 1949) shows that the acceleration variance is given by

$$\langle a^2 \rangle = a_0 \varepsilon^{3/2} v^{-1/2}, \quad (7)$$

where  $a_0$  is assumed to be a universal constant (approximately 6 at high Reynolds numbers, Voth *et al* (2002)). For our cloud  $\langle a^2 \rangle \sim 70 \text{ m}^2 \text{ s}^{-4}$ , i.e. the characteristic acceleration of an inertia-less fluid particle will be approximately  $8 \text{ m s}^{-2}$ , the order of the gravitational acceleration. But the Kolmogorov 1941 scaling does not take into account the intermittent nature of the turbulence.

Since the late 1940s it has been recognized that the velocity field (and also any passive admixture) exhibits small-scale intermittency (Frisch 1995) characterized by strong variability in the dissipation (and mixing) rates (see figure 2, Warhaft 2000). Although the velocity spectrum requires only slight modification as a result of intermittency, the higher movements are significantly affected (Frisch 1995). Thus, fluctuations at the small scale are much greater than would be predicted from a Gaussian distribution. The dissipation rate itself now becomes a fluctuating variable. We replace  $\varepsilon$  with  $\varepsilon_r$ , a local value averaged over a sphere of radius  $r$ . There is at present no fully deductive theory, using the Navier–Stokes equations as the basis to provide the statistical distribution of  $\varepsilon_r$  (Frisch 1995, Kida 1991), but data suggest that it can be reasonably modeled as log-normally distributed; i.e.  $\ln(\varepsilon_r/\varepsilon)$  is a Gaussian distribution (Kolmogorov 1962). An extra length scale needs to be employed in order to do the scaling. Kolmogorov (1962), using the integral scale,  $\ell$ , as the additional scale, assumed that the mean square dissipation fluctuations scale as

$$\langle \varepsilon_r^2 \rangle / \varepsilon^2 \sim (\ell/\eta)^\mu, \quad (8)$$

where  $\mu$  is known as the intermittency exponent. From (7) and the log-normal assumptions (Pope 2000) it follows that

$$\langle a^2 \rangle = a_0 \varepsilon^{3/2} v^{-1/2} (\ell/\eta)^{3\mu/8}. \quad (9)$$

From estimates of the turbulence kurtosis, it can be deduced (Pope 2000) that  $\mu \sim 0.25$ . Further, from equations (3), (5) and (6), it follows that  $\ell/\eta \sim R_\lambda^{3/2}$  and  $\langle a^2 \rangle / \varepsilon^{3/2} v^{-1/2} \sim R_\lambda^{0.14}$ . Because of intermittency, the acceleration variance is a function of Reynolds number and it follows that  $a_0$  (equation (9)) cannot be a universal constant. We note that the dependency of  $\langle a^2 \rangle$  on Reynolds number has yet to be verified experimentally (for attempts, see Gylfason *et al* 2004, Voth *et al* 2002), although there has been confirmation using DNS (Ishihara *et al* 2007, Vedula and Yeung 1999), up to  $R_\lambda \sim 1000$ . The intermittency correction for the variance (compare equations (7) and (9)) increases the variance by a factor of 3 for our typical cloud. But we will show that there are rare events with extremely high instantaneous accelerations, and this has significant consequences for raindrop growth.



#### 4. Laboratory experiments on the tracking of particles in turbulence

Clouds consist of droplets in turbulent motion. In order to predict the droplet growth it is first necessary to understand how particles move and coalesce in turbulent flows. Thus, we need to use the Lagrangian approach to track the particles. Consider a table top experiment using water (which has a lower kinematic viscosity than that of air ( $\nu = 10^{-6} \text{ m}^2 \text{ s}^{-1}$ ), and therefore higher Reynolds number can be achieved) in a stirred tank to be discussed in more detail below. Here,  $\ell$  is typically 0.1 m and  $\langle u^2 \rangle^{1/2}$  is approximately  $1 \text{ m s}^{-1}$ . Thus,  $\varepsilon$  is approximately  $10 \text{ m}^2 \text{ s}^{-3}$ . From (6) it follows that  $\tau_\eta$  is 0.3 ms. To track particles, timescales must ideally be resolved to an order of magnitude smaller than this:  $\tau_\eta$  is the peak small characteristic timescale but there is activity at smaller timescales. Moreover, the characteristic small length scale,  $\eta$ , is  $18 \mu\text{m}$ . These considerations imply that to capture the tracks of particles in turbulence, and thereby determine the Lagrangian statistics, very fast tracking devices are needed.

In the mid-1990s Eberhard Bodenschatz, a professor of physics at Cornell, and his student, Greg Voth realized that detectors used in high energy particle physics may be useful in tracking fluid particles (La Porta *et al* 2001, Voth *et al* 2002). Previous work on Lagrangian tracking had been hampered by inadequate temporal resolution and had been limited to low Reynolds numbers (Ott and Mann 2000, Sato and Yamamoto 1987, Snyder and Lumley 1971). Bodenschatz and his group adapted strip detectors, which were being used to measure the tracks of sub-atomic particles at the Cornell Electron–Positron Collider. This half mile-circumference collider is used to examine the ‘Standard Model’ describing elementary particles and their reactions. The objective of the experiment, known as CLEO (<http://www.lepp.cornell.edu/research/EPP/CLEO/>), in which the strip detectors are used, is to elucidate the physics of charm and bottom quark decays. This experiment indicates the extreme abstraction that has occurred since the early beginnings of detector physics. Yet, in common with its humble origins, tracks of particles are measured. But here the detector has little resemblance to the photographic method employed by C T R Wilson a century ago.

The silicon strip detectors adapted by the Bodenschatz group consist of a large planar photodiode, segmented into 512 sensing strips. A laser beam illuminates small spheres in the turbulence chamber and the resulting scattered radiation creates electron–hole pairs at the detector. The charge collected by the array of strips gives a one-dimensional (1D) projection of the incident light and one coordinate of a particle can be determined. By measuring primary and conjugate peaks each detector can measure two components of velocity and two separate detectors are used to determine the 3D motion. The temporal resolution of the detector is 70 000 frames per second allowing for resolution of the smallest scales. A combination of lenses images the fluid volume of interest onto the detectors. The test chamber is cylinder filled with water. At the top and bottom there are counter rotating discs of diameter 20 cm with 33 cm spacing between them. This is a table top experiment (figure 5) in the spirit of Aitkin and C T R Wilson (section 2). The discs create highly turbulent fluid up to an  $R_\lambda$  of approximately 1000. Figure 6 shows typical tracks. These tracks are reminiscent of the tracks of Wilson, but the reason for them could not be more different. Here, the focus is on neutral particles. Their trajectory is determined by the fluid motion itself.

Figure 7 shows that the probability density function (pdf) of fluid particle acceleration has very broad, exponential tails due to the highly intermittent nature of the turbulence. ‘Gusts’ where the rms may be as much as 20 times greater than the gravitational acceleration,  $g$ , occur although the rms is only of the order of  $g$ . It is important to note that the acceleration pdf reflects the small-scale activity. At the large scale, the turbulence is approximately Gaussian.

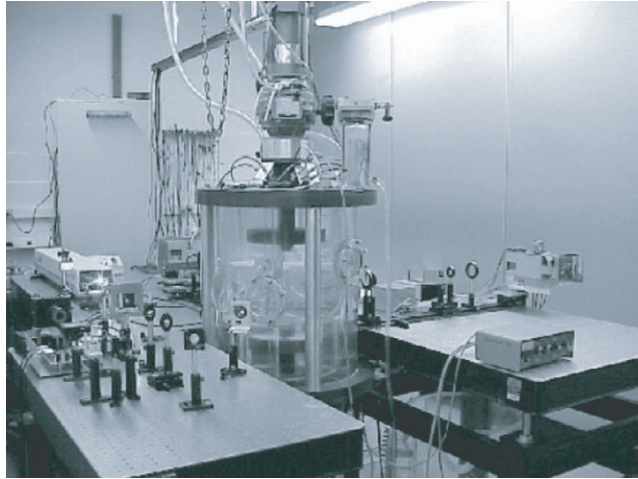


**Figure 5.** The Bodenschatz table-top turbulence experiment used to study particle trajectories in a swirling turbulent flow. The distance between the rotating discs in the plexiglass-water filled-container is 33 cm. An  $R_\lambda$  of approximately 1000 was achieved in this small apparatus. Image taken from Voth *et al* (2002). Copyright 2002, Cambridge University Press.

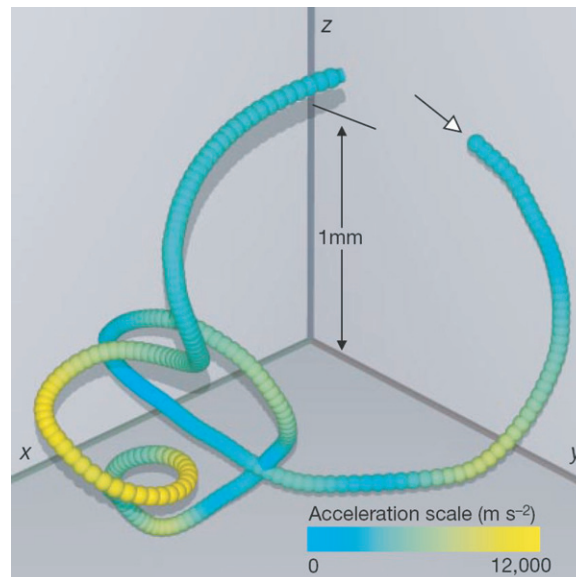


**Figure 6.** 3D time-resolved particle tracks in high Reynolds number turbulence, produced by the apparatus in figure 5. The acceleration magnitude is represented by the color of the trajectory. Accelerations as high as  $12\,000\text{ ms}^{-2}$  are observed. Image taken from La Porta *et al* (2001). Reprinted by permission from Macmillan Publishers Ltd: Nature, Copyright 2001.

The results of the Bodenschatz group are consistent with another novel experiment, that of Jean-Francois Pinton and his co-workers in Lyon (Mordant *et al* 2001). Counter rotating discs were used to create turbulence in a bench-top apparatus, similar to that of Bodenschatz, but in the Pinton experiment ultrasonic techniques were used to track the fluid particles. In this experiment, the particle size was greater than the Kolmogorov scale ( $d/\eta \sim 17$ ). Hence,

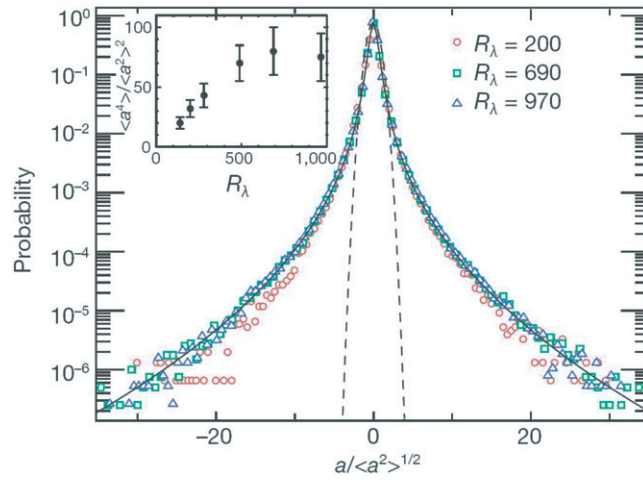


**Figure 7.** The pdf of the transverse acceleration of fluid particles, normalized by its standard deviation. The dashed line is a Gaussian distribution with the same variance. The wide tails are the result of the intense, intermittent acceleration events (figure 6). The inset shows the normalized fourth moment of the acceleration. Estimates using intermittency models predict that this should grow with increasing  $R_\lambda$ . Image taken from La Porta *et al* (2001). Reprinted by permission from Macmillan Publishers Ltd: Nature, Copyright 2001.

the dissipation scales could not be resolved. Here, the focus was on the inertial subrange. Stretched tails, indicating pronounced intermittency, were observed in their velocity increment pdfs, similar to those observed by the Bodenschatz group.

## 5. The formation of raindrops

The Bodenschatz experiment tracked ‘fluid particles,’ small, sub-Kolmogorov particles that have the same density as that of the fluid, and therefore follow the fluid motion. Raindrops have a density 1000 times that of the surrounding air and thus we would expect that inertial effects would play a role in their motion. The heavy water particles, known as inertial particles, will be ejected by the centrifugal forces from regions of high vorticity (where there is strong dissipation) and accumulate in regions of high strain (Eaton and Fessler 1994, Maxey and Riley 1983, Shaw 2003, Shaw and Oncley 2001, Squires and Eaton 1991, Sundaram and Collins 1997). This has the effect of causing the droplets to cluster: a uniform distribution of particles placed in a turbulent flow will tend to congregate in regions of high strain, i.e. at scales of the order of the Kolmogorov scale. This has been born out by numerical simulations (Sundaram and Collins 1997). The multiscale nature of turbulence can also promote clustering at the larger scales (Chen *et al* 2006, Yoshimoto and Goto 2007). We will provide experimental evidence of clustering below. Because the droplet collision rate is proportional to the square of the number of particles (Pruppacher and Klett 1997, Shaw 2003), the clustering may enhance droplet growth rate and hence rain formation.

Inertial effects are described by the Stokes number  $St = \tau_p / \tau_\eta$  where  $\tau_p$  is the particle inertial response time and  $\tau_\eta$  (equations (6)) is the timescale of the smallest eddies. It is these eddies that have the most intense accelerations and thus they will have the strongest effect on the motion of the inertial particles. The particle inertial response time is defined as  $\tau_p = (1/18)[\rho_p / \rho_f]d^2 / \nu$ , where  $\rho_p$ ,  $\rho_f$ ,  $d$  and  $\nu$  are, respectively, the particle density, fluid density, particle diameter and fluid viscosity (Pruppacher and Klett 1997), and thus, using the

second of relations (6)

$$St \equiv \frac{\tau_p}{\tau_\eta} = \frac{1}{18\nu^{3/2}} \frac{[\rho_p - \rho_f]}{\rho_f} d^2 \varepsilon^{1/2}. \quad (10)$$

For water drops in air,  $St \propto d^2 \varepsilon^{1/2}$ .

Inertial effects become significant at  $St$  as low as 0.01 (Chun *et al* 2005), and as the Stokes number increases the effects grow and then diminish for  $St$  greater than unity (see Wood *et al* 2005). Nevertheless clustering is observed for  $St$  as large as 10 and at scales significantly larger than the Kolmogorov scale. The Wood *et al* (2005) experiments show clustering in the inertial subrange and this is also observed in the experiments of Saw *et al* (2008); see figure 11 below.

Traditional models of raindrop formation (Pruppacher and Klett 1997, Rogers and Yau 1989) under predict the droplet growth rate, which can be as short as 15 min after the cloud begins to form. Classical theory has the condensation occurring on aerosol nuclei, typically growing from the submicron size of the nuclei to around  $10 \mu\text{m}$  by the process of condensation. Because the droplet growth rate by condensation is inversely proportional to the droplet radius, the droplet size distribution narrows during condensation. Further growth of droplets by means of collision and coalescence occurs as they fall through the cloud at their terminal speed. Larger drops, falling at a greater velocity overtake the small ones and thereby grow by collision and coalescence. The classical theory, based on gravitational coalescence, is unable to produce the rapid rate of size increase in droplets in part because the droplet size distribution is not broad enough to begin with. The collision kernel, the expected time for a droplet to experience a collision with another droplet of a different size, is strongly related to the particle size distribution (Shaw 2003) and to the accelerations of the particles. In the classical theories, the acceleration due to the turbulence is neglected.

The role of turbulence may be critical in enhancing the condensation and the collision coalescence process. The small scales of turbulence experience large accelerations at high Reynolds number and as we have shown (figure 7), these will be greater than the gravitational acceleration. Further, the structure of the turbulence allows for cloud particles to preferentially concentrate as a result of their inertia. This may increase the size distribution of the condensation phase by inducing vapor supersaturation fluctuations (Shaw *et al* 1998a,b) and at the coalescing stage by increasing the collision efficiency (Reade and Collins 2000).<sup>2</sup> All these issues are linked because of the multiscale nature of turbulence.

In order to study the effect of turbulence on inertial particles, we have employed a large ( $1 \text{ m} \times 0.9 \text{ m} \times 20 \text{ m}$ ) open circuit wind tunnel with an active grid (triangular agitator wings attached to the rotating grid bars, randomly flipping (Makita 1991, Mydlarski and Warhaft 1996)) to produce turbulence in the range  $100 \leq R_\lambda \leq 1000$ . The water spray consists of an array of four nozzles symmetrically placed downstream of the grid (figure 8). The particle drop size was measured using a phase Doppler particle sizer (Ayyalasomayajula *et al* 2006). The particle mass loading was approximately  $10^{-4} \text{ kg water kg}^{-1} \text{ dry air}$ . A high speed camera (Phantom v7.1) attached to a precision linear motion pneumatic-driven sled was accelerated to the mean flow speed and 2D particle tracks were measured at region 30 mesh lengths ( $M = 11.4 \text{ cm}$ ) downstream from the grid and 20.3 cm from the tunnel wall. The camera frame rate was 8000 fps with a resolution of  $512 \text{ pixels} \times 512 \text{ pixels}$ . The laser light sheet (Nd-YAG, 20W, pulse width 120 ns at a repetition rate of 40 kHz) was projected from the top of the tunnel such that the camera received light forward scattered at an angle of  $30^\circ$ . The width of

<sup>2</sup> Kostinski and Shaw (2005) have emphasized the importance of fluctuations in droplet growth by focusing on very rare ‘lucky’ fast or giant droplets that may initiate the rain in warm clouds.

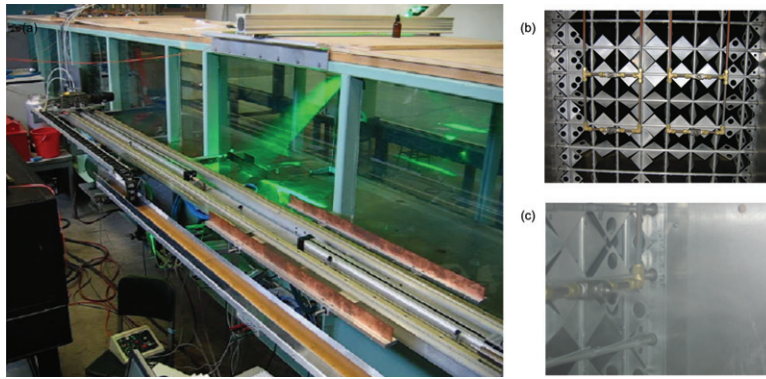


**Figure 8.** The wind tunnel in the DeFrees laboratory at Cornell used to study inertial particles in high Reynolds number turbulence; (a) the plexiglass-open circuit-tunnel ( $1 \text{ m} \times 0.9 \text{ m} \times 20 \text{ m}$ ) showing the camera (far left, at the beginning of its trajectory), the sled and the laser sheet. (b) The active grid (used to generate high Reynolds number turbulence) and (c) the spray system. They are located at the far left of (a).

the sheet was 2 mm. The sampling area was  $1.9 \times 1.9 \text{ cm}^2$ , the inter-sample time was  $(1/100)\tau_\eta$  and the spatial resolution was  $(1/12)\eta$ . The camera tracked the particles over a distance of 40 cm (0.2 s) as they moved across the light sheet. Approximately 15 000 data points were taken per sled run, and 400 runs were completed to provide  $6 \times 10^6$  data points per set.

Figure 9 shows the normalized pdf of the longitudinal component of the acceleration of inertial particles compared with those of fluid particles. There are two related effects due to the inertia: the acceleration variance decreases as a result of the linear damping of the fluid acceleration, and the pdf tails become narrower. The first effect is not shown because the pdf is normalized. The narrowing of the tails is a result of biased sampling of the underlying fluid flow due to inertia. The inertial particles will experience events of varying magnitude due to the intermittent structure of the flow field. Evidently the effects of very large acceleration events that we can associate with the intense vorticity of the turbulence are attenuated, reducing the width of the tails. Thus, there is a relationship between the acceleration pdf and the clustering mechanisms.

In order to elucidate the relationship between the acceleration pdf and the clustering, we developed a new model that uses an array of potential vortices to simulate a 2D flow in which fluid particles and inertial particles are tracked to obtain Lagrangian velocities and accelerations (Ayyalasomayajula 2007, Ayyalasomayajula *et al* 2008). In contrast with earlier stochastic models (Reynolds 2003, Sawford 1991), this model allows the inertial particles to choose the fluid field it wishes to sample. An array of ten-by-ten vortices was used, separated by a distance  $L$  (figure 10) which we call the integral scale. The flow field around a vortex was obtained using the 2D potential theory but to prevent infinite velocity near the center of each vortex, a viscous-like core with radius  $s$  was added. Here,  $s$  acts like a small-scale turbulence length scale. The circulation of each of the vortices  $\Gamma_i$  was set using an independent Gaussian random variable whose mean is zero and standard deviation is  $\sigma_\Gamma$ . To mimic the persistence of large-scale eddies as in the real turbulent flow, the circulation was randomly updated at a timescale,  $T$ . The timescale  $T$  is associated with the slowest eddies of size  $L$  and the timescale is constructed as  $L^2/\sigma_\Gamma$ . Similarly a small-scale time  $t_s$  is constructed as  $s^2/\sigma_\Gamma$  and it can be related to the most rapid changes in the flow, which are occurring close to the core of the vortex where maximum induced velocity is expected. The inertial particle has one-way coupling to



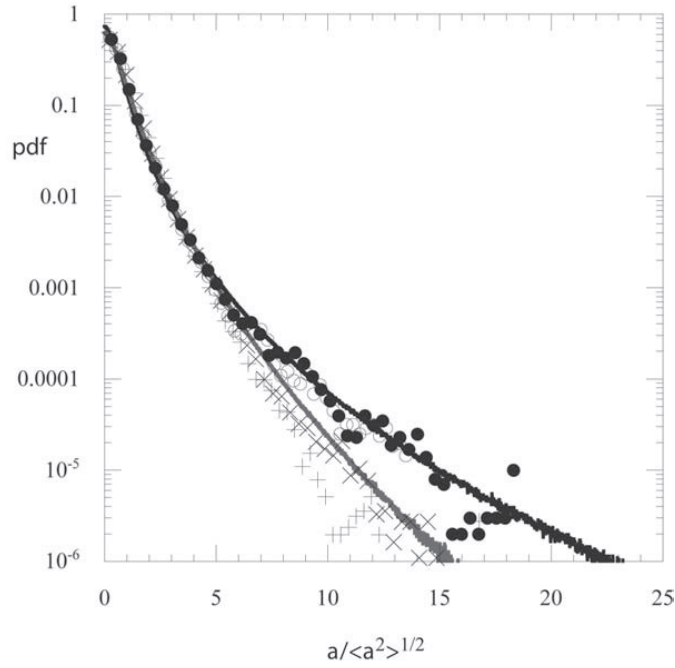


**Figure 9.** The normalized pdfs of the longitudinal components of the acceleration of inertial water particles ( $St = 0.09$ ,  $\times$ ;  $St = 0.15$ ,  $+$ ) compared with passive particles (filled circles) measured in the Cornell wind tunnel  $R_\lambda = 250$ . Also shown are the DNS results at comparable  $R_\lambda$  and  $St$ , from Bec *et al* (2006). Black line, DNS of fluid particles; gray line, DNS of inertial particles;  $St = 0.16$ . For both cases  $R_\lambda = 185$ .

the flow through Stokes drag. The acceleration of the particle was obtained from the material derivative ( $D\mathbf{v}(t)/Dt$ ) of the inertial particle velocity. The Stokes number  $St$  for this model is defined as the ratio of particle response time,  $\tau_p$  and the flow timescale,  $t_s$ .

The simple vortex model exhibits the stretched exponential tails for the acceleration pdf that is observed in the data (figure 10(b)). It also produces clustering away from the vortex centers (figure 10(c)) due to the selective sampling of the fluid by the inertial particles, and this is correlated with the narrowing of the shape of the pdf. Ayyalasomayajula (2007) and Ayyalasomayajula *et al* (2008) also computed the Lagrangian acceleration auto-correlation function, conditioned on the magnitude of the acceleration, for the fluid along an inertial particle trajectory, and showed that as the magnitude of the acceleration increases, the correlation time decreases. Thus inertial particles with high acceleration are ‘filtered’ because their response time to the turbulence is too short. This has the effect of excluding extreme acceleration events, thereby narrowing the inertial particle pdf tails. By computing the fluid acceleration conditioned on the inertial particle acceleration Ayyalasomayajula (2008) also showed that for small  $St (< 0.5)$  the inertial particle acceleration coincides with that of the fluid acceleration, but because the inertial particles are not homogeneously distributed, concentrating in regions of low vorticity (clustering), the inertial particle variance is reduced due to the preferential concentration. This is consistent with the numerical study of Bec *et al* (2006). Thus, there is a clear link between the acceleration pdf and the clustering and filtering of the inertial particles. The relative effects of the two mechanisms: clustering and filtering, need further study. In the Bec *et al* (2006) DNS, clustering dominates but in the vortex model filtering is also significant, although clustering dominates at very low

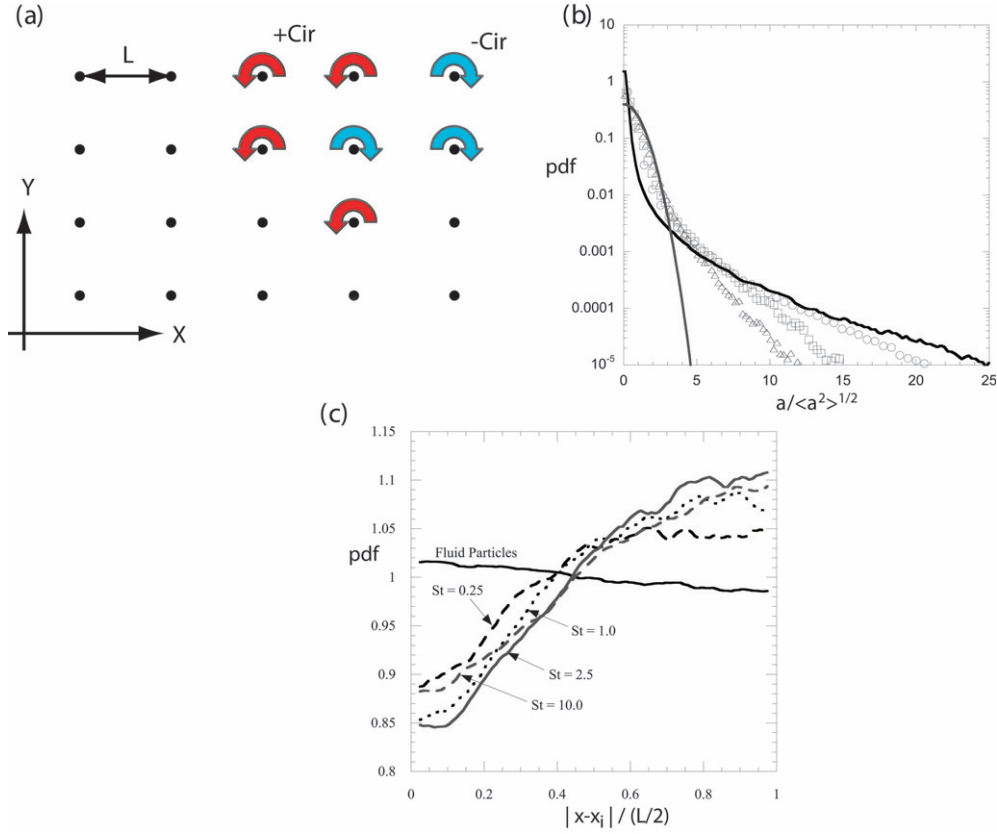


**Figure 10.** A vortex model used to mimic inertial particles in a random flow. (a) The model consists of a  $10 \times 10$ -2D array of evenly spaced vortices which randomly vary in direction.  $L$  is the distance between vortices. (b) The pdf of the normalized acceleration for the fluid particles. As for the experiments, the model reproduces the stretched exponential tails (circles, squares and triangles) and they become narrower as the  $St$  increases. The gray line is a Gaussian pdf. (c) pdfs of the location of particles from vortex center. As the Stokes number increases there is less and less probability of finding a particle at the vortex center. From Ayyasomayajula *et al* (2008).

Stokes number. Further experimental study of this problem is needed. Apart from the issue of understanding inertial particle behavior in its own right, the investigation of inertial particles is telling us about the fluid structure itself and is therefore a valuable diagnostic tool. There is much to do in this fertile area.

Recently, there have been a number of laboratory studies of the clustering of inertial particles (Salazar *et al* 2008, Saw *et al* 2008, Wood *et al* 2005). Clustering may be described in terms of the radial distribution function (rdf) (Shaw *et al* 2002, Sundaram and Collins 1997) defined as

$$g(r) = \left\langle \frac{\rho_p(r)}{\rho_p} \right\rangle, \quad (11)$$

where  $\langle \rho_p(r) \rangle$  is the particle density at a distance  $r$  relative to each particle, averaged over all particles, and  $\rho_p$  is the global particle density. If there is no clustering,  $g(r) = 1$ . We would expect that when clustering occurs,  $g(r)$  will peak in the dissipation range, since it is here that the regions of maximum strain (velocity gradient) occur.



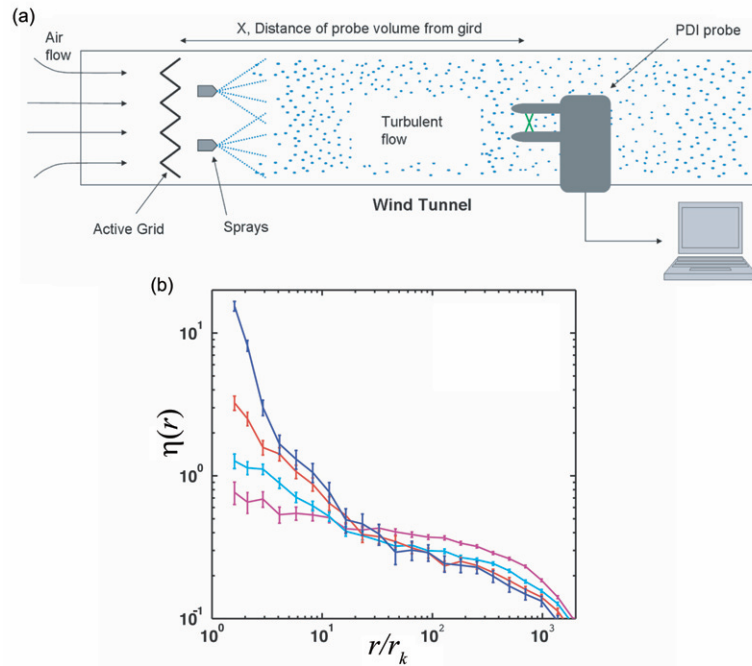


**Figure 11.** Measurements of the pair correlation of inertial particles in the Cornell tunnel. (a) The experimental setup showing the phase Doppler interferometer for measuring the 1D rdf from their time of arrival (top panel). (b) The pair correlation functions for various Stokes numbers. The high values at dissipation scales ( $r \sim r_k$ , where  $r_k$  is the Kolmogorov scale) indicate clustering, which increases as  $St$  increases from the bottom graph ( $St = 0.01$ – $0.3$ ) to the top ( $St = 1.1$ – $1.5$ ). The intermediate values are  $0.3$ – $0.7$  and  $0.7$ – $1.1$ . The Taylor–Reynolds number range was  $440$ – $590$ . Images taken from Saw *et al* (2008). Copyright 2008, American Physical Society.

In the Cornell tunnel discussed above, Saw *et al* (2008) used a phase Doppler interferometer downstream of the active grid and spray system and obtained an estimate of the 1D rdf from time of arrival measurements. They found significant clustering at the dissipation scales where the fluid acceleration is at its maximum. A plot of the pair correlation function  $\eta(r) \equiv g(r) - 1$  is shown in figure 11. Note that although the clustering peaks at the small scales, it persists to larger (inertial) scales. As the Stokes number increases, so does the magnitude of the clustering. The figure also shows Stokes number similarity for droplets of different diameters. The trend of these results is seen in the work of Wood *et al* (2005) and Salazar *et al* (2008) in completely different experimental apparatus. In these experiments, a turbulence box was used: fans at the corners of a box produce the turbulence which, at the center where the measurements are made, is approximately isotropic. Salazar *et al* compare their measurements with DNS and find satisfactory agreement (figure 12). Other laboratory experiments using Eulerian methods to investigate preferential concentration include the work of Aliseda *et al* (2002) and the earlier work of Wells and Stock (1983). Vohl *et al* (1999) study the growth of single droplets by collision coalescence in a wind tunnel. They compare laminar and turbulent flows and their preliminary results suggest that the droplet growth rate is faster under turbulent conditions. An important issue that needs systematic study is the dependency of clustering on Reynolds number. Numerical results (Collins and Keswani 2004) indicate saturation of the rdf as the Reynolds number is increased. However, the DNS is for a limited range of Reynolds numbers.

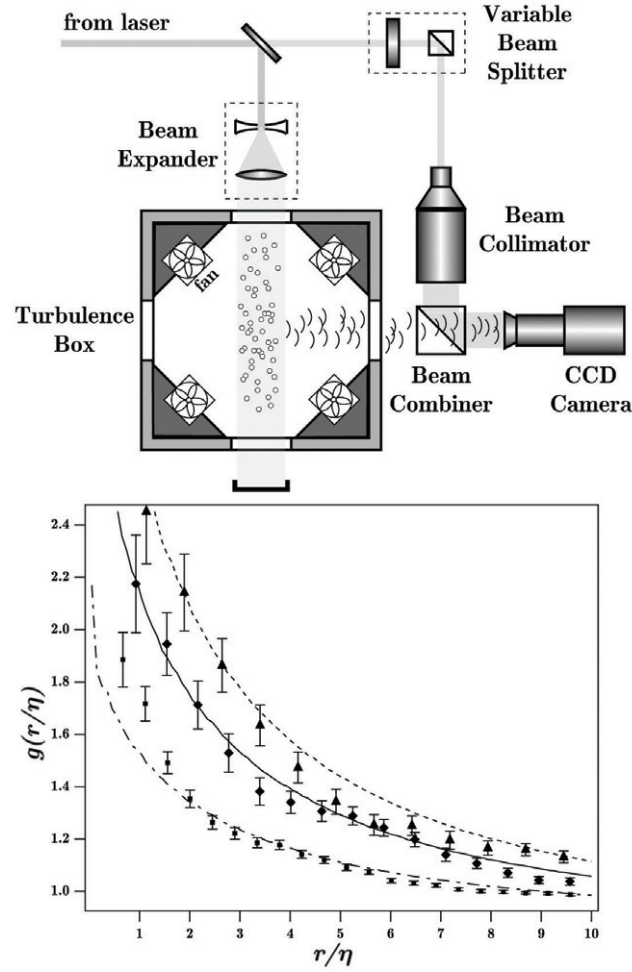


**Figure 12.** Measurements of the 3D rdf in a turbulence box. (a) Schematic of the turbulence box and holographic imaging setup. The particles used were hollow glass spheres (top panel). (b) The rdf. The mean Stokes number increases from  $St = 0.21$  (lower most curve) to  $St = 0.40$  and  $St = 0.60$  (upper curve). The Taylor–Reynolds number range was 108–147. The dashed and full lines are DNS of the experiments. The results are in qualitative agreement with those of Saw *et al* (figure 11) but quantitative comparison is difficult since these are 3D (volume) measurements. Those of Saw *et al* are time of arrival 1D measurements. Image taken from Salazar *et al* (2008). Copyright 2008, Cambridge University Press.

Experiments have been conducted in the atmosphere too. Here, the resolution is much poorer but there is evidence that clustering is occurring at the smallest scales. Lehman *et al* (2007), using a tethered balloon, measured the pair distribution function in a stratus cloud in which the Stokes number was gradually varying. The Stokes number was determined by measuring droplet size and local energy dissipation rate (see relation following equation (10)). They found that clustering was positively correlated with the droplet  $St$  and they infer that the droplet collision rate depends not only on the droplet size distribution, but also on the turbulence level. Earlier work by Uhlig *et al* (1998) and by Pinsky and Khain (2003) are not inconsistent with these results. In an ambitious experiment, Bodenschatz proposes using a sled mechanism with high speed cameras (similar to the setup in figure 8(a)) to measure



**Figure 13.** The Schneeferner Haus on the Zugspitz, Germany's highest mountain, a possible site proposed by E Bodenschatz to do Lagrangian experiments of cloud particles, *in situ*.

cloud particles on the side of the Zugspitz, Germany's highest mountain (figure 13). Such an experiment is very much in the spirit of the early work of J Aitkins and C T R Wilson referred to in section 2 (figure 4). By moving back and forth between the laboratory and the field using the same apparatus, the gap between the abstract and mimetic experiments will inevitably narrow.

## 6. Concluding comments

In this review, I have described recent developments in experimental methods used for the study of particles in turbulent flows. I have focused on Lagrangian techniques, where the frame of reference moves with the fluid particle. By these means the temporal evolution of the turbulent flow field can be determined, and thereby fundamental insights into particle motion can be gained.

The new experiments described here provide the beginnings that will lead to a better understanding of droplet formation in clouds. Further work will include systematic studies of clustering as a function of Reynolds number to determine whether saturation of the clustering occurs at high Reynolds number. The effects of long range interaction between the large and small scales (Warhaft 2002 and references there in) on clustering needs examination, as do the effects of Reynolds and Stokes numbers on clustering at the larger scales. The way particle pair dispersion is affected by the inertia of the particles also needs investigation. Particle size effects need to be studied<sup>3</sup>. The experiments mentioned above are for particles smaller than the Kolmogorov scale. And the particle concentrations need to be systematically varied so that collisions can be introduced into the experiments. Experiments in inhomogeneous flows are also needed. We have no evidence of how the inertial particle acceleration pdf and the radial distribution vary in inhomogeneous flows. Experiments also need to move to a parameter range that is closer to that observed in clouds. In warm cumulous clouds,  $St$  is in the range  $10^{-3}$ – $10^{-1}$ , and the dissipation rate is low, typically of the order of  $10^{-2} \text{ m}^2 \text{ s}^{-3}$  (much lower than usually observed in experiments), but it can vary by orders of magnitude. The highest Taylor Reynolds number presently obtained in experiments is of the order of  $10^3$ , whereas in clouds it can range from  $10^4$  to  $10^5$ . Gravitational effects also need to be systematically

<sup>3</sup> See Qureshi *et al* (2007) and Xu and Bodenschatz (2008) for recent advances in this area.

studied in the laboratory. In this review, we have stressed the statistical nature of the subject and the importance of rare events in determining clustering. Classical theory ([Ruppacher and Klett 1997](#)) is unable to explain the rapid rain initiation time observed in clouds: the statistical nature of the turbulence may provide a key element in understanding the enhanced collision rates needed for the rapid droplet growth. The subject is burgeoning and significant advances can be expected in the next few years.

I have also drawn attention to the interesting history of the subject. Clouds and droplets have been studied in the laboratory for more than a century. It was the early droplet studies of C T R Wilson that led to the development of the particle detectors that are used today in high energy physics. In an interesting turnabout, these modern particle detectors have recently been used to study the Lagrangian properties of fluid particles (figure 6). I think that C T R Wilson would have been pleased to see the return to the study of droplet formation in the laboratory in this way.

Finally, I have discussed the dichotomy between abstract and mimetic experiments: the reductionist and the holistic approach. Whether, by means of clever experiments, theory and computation we will be able to build up a cloud, with all its complexity, from an understanding of its component parts, or whether a more synthetic approach is needed, remains an open question. We note that the fractal approach has been successful in describing clouds and there is considerable literature on the subject (e.g. [Cahalan and Joseph 1989](#), [Sachs et al 2002](#)). Whether this approach will lead to an understanding, in the way that experiments or DNS does, is not clear. So far the main contribution of the fractal approach has been to provide a description. It does not provide the understanding that comes from the Navier–Stokes equations, which are thought to incorporate the full dynamics of the turbulent field. What is required is a holistic approach that provides insight into the dynamics, and provides predictions of the rate of drop formation, and other important characteristics.

## Acknowledgments

I thank Lance Collins and Raymond Shaw for discussions and for the data of figures 11 and 12, and Laurent Mydlarski for comments on an earlier draft. I also thank Sathya Ayyalasomayajula, June Meyermann and Gabriel Terrizzi for help with the manuscript. This work was funded by a grant from the US National Science Foundation.

## References

- Aitken J 1923 *Collected Scientific Papers* ed C G Knott (Cambridge: Cambridge University Press)
- Aliseda A, Cartellier A, Hainaux F and Lasheras J C 2002 Effect of preferential concentration on the settling velocity of heavy particles in homogeneous isotropic turbulence *J. Fluid Mech.* **468** 77–105
- Ayyalasomayajula S, Gylfason A, Collins L R, Bodenschatz E and Warhaft Z 2006 Lagrangian measurements of inertial particle accelerations in grid generated wind tunnel turbulence *Phys. Rev. Lett.* **97** 144507
- Ayyalasomayajula S 2007 Experimental Eulerian and Lagrangian investigations in simple turbulent flows *PhD Thesis* Cornell University, Ithaca, NY
- Ayyalasomayajula S, Collins L R and Warhaft Z 2008 Modelling inertial particle Lagrangian acceleration statistics in turbulent flows *Phys. Fluids*. **20** 095104
- Bec J, Biferale L, Boffetta G, Celani A, Cencini M, Lanotte A, Musacchio S and Toschi F 2006 Acceleration statistics of heavy particles in turbulence *J. Fluid Mech.* **550** 349
- Bourgoin M, Ouellette N T, Xu H T, Berg J and Bodenschatz E 2006 The role of pair dispersion in turbulent flow *Science* **311** 835–8
- Cahalan R F and Joseph J H 1989 Fractal statistics of cloud fields *Mon. Weather Rev.* **117** 261–72
- Cencini M, Bec J, Biferale L, Boffetta G, Celani A, Lanotte A S, Musacchio S and Toschi F 2006 Dynamics and statistics of heavy particles in turbulent flows *J. Turbul.* **7** 1–16

- Chen L, Goto S and Vassilicos J C 2006 Turbulent clustering of stagnation points and inertial particles *J. Fluid Mech.* **553** 143–54
- Chun J H, Koch D L, Rani S L, Ahluwalia A and Collins L R 2005 Clustering of aerosol particles in isotropic turbulence *J. Fluid Mech.* **536** 219–51
- Collins L R and Keswani A 2004 Reynolds number scaling of particle clustering in turbulent aerosols *New J. Phys.* **6** 119
- Cristini V, Blawdziewicz J, Loewenberg M and Collins L R 2003 Breakup in stochastic Stokes *J. Fluid Mech.* **492** 231–50
- Eaton J K and Fessler J R 1994 Preferential concentration of particles by turbulence *Int. J. Multiph. Flow* **20** (suppl) 169–209
- Falkovich G and Pumir A 2004 Intermittent distribution of heavy particles in a turbulent flow *Phys. Fluids* **16** L47–50
- Franklin C N, Vaillancourt P A, Yau M K and Bartello P 2005 Collision rates of cloud droplets in turbulent flow *Source J. Atmos. Sci.* **62** 2451–66
- Frisch U 1995 *Turbulence: The Legacy of A.N. Kolmogorov* (Cambridge: Cambridge University Press)
- Galison P 1997 *Image and Logic* (Chicago, IL: University of Chicago Press)
- Gylfason A, Ayyalasomayajula S and Warhaft Z 2004 Intermittency, pressure and acceleration statistics from hot-wire measurements in wind-tunnel turbulence *J. Fluid Mech.* **501** 213–29
- Hamblyn R 2001 *The Invention of Clouds* (New York: Picador Press)
- Hamilton J 1998 *Turner and the Scientists* (London: Tate Gallery Publishing)
- Heisenberg W 1948 Zur statischen theorie der turbulenz *Z. Phys.* **124** 628–57
- Ishihara T, Kaneda Y, Yokokawa M, Itakura K and Uno A 2007 Small-scale statistics in high-resolution direct numerical simulation of turbulence: Reynolds number dependence of one-point velocity gradient statistics *J. Fluid Mech.* **592** 335–66
- Kerstein A R and Krueger S K 2006 Clustering of randomly advected low-inertia particles: a solvable model *Phys. Rev. E* **73** 025302 2
- Kida S 1991 Limitation of log-normal theory of turbulence *Phys. Soc. Japan* **60** 477–80
- Kolmogorov A N 1941 The local structure of turbulence in an incompressible fluid at very high Reynolds numbers *Dokl. Akad. Nauk SSSR.* **30** 299–303
- Kolmogorov A N 1962 A refinement of previous hypotheses concerning the local structure of turbulence in a viscous incompressible fluid at high Reynolds number *J. Fluid Mech.* **13** 82
- Kostinski A B and Shaw R A 2005 Fluctuations and luck in droplet growth by coalescence *Bull. Am. Meteorol. Soc.* **86** 235
- Lamb H 1995 *Climate, History and the Modern World* (London: Routledge) p 249
- La Porta A, Voth G A, Crawford A M, Alexander J and Bodenschatz E 2001 Fluid particle accelerations in fully developed turbulence *Nature* **409** 1017–9
- Lehmann K, Siebert H, Wendisch M and Shaw R A 2007 Evidence for inertial droplet clustering in weakly turbulent clouds *Tellus B* **59** 57–65
- Makita H 1991 Realization of a large-scale turbulence field in a small wind-tunnel *Fluid Dyn. Res.* **8** 53–64
- Maxey M R and Riley J J 1983 Equation of motion for a small rigid sphere in a non-uniform flow *Phys. Fluids* **26** 883
- Mordant N, Metz P, Michel O and Pinton J F 2001 Measurement of Lagrangian velocity in fully developed turbulence *Phys. Rev. Lett.* **87** 214501
- Mydlarski L and Warhaft Z 1996 On the onset of high-Reynolds-number grid-generated wind tunnel turbulence *J. Fluid Mech.* **320** 331–68
- Ott S and Mann J 2000 An experimental investigation of the relative diffusion of particle pairs in three-dimensional turbulent flow *J. Fluid Mech.* **422** 207–23
- Pinsky M and Khain A 2003 Fine structure of cloud droplet concentration as seen from the fast-FSSP measurements. Part II: results of *in situ* observations *J. Appl. Meteorol.* **42** 65–73
- Pinsky M B and Khain A P 2004 Collisions of small drops in a turbulent flow. Part II: effects of flow accelerations *J. Atmos. Sci.* **61** 1926–39
- Pope S B 2000 *Turbulent Flows* (Cambridge: Cambridge University Press)
- Pruppacher H R and Klett J D 1997 *Microphysics of Clouds and Precipitation* 2nd edn (Dordrecht: Kluwer)
- Qureshi N M, Bourgoin M, Baudet C, Cartellier A and Gagne Y 2007 Turbulent transport of material particles: An experimental study of finite size effects *Phys. Rev. Lett.* **99** 184502
- Reade W C and Collins L R 2000 Effect of preferential concentration on turbulent collision rates *Phys. Fluids* **12** 2530–40
- Reynolds A M 2003 On the application of nonextensive statistics to Lagrangian turbulence *Phys. Fluids* **15** L1–4
- Richardson L F 1926 Atmospheric diffusion shown on a distance-neighbor graph *Proc. R. Soc. A* **90** 709–73

- Riemer N, Wexler A S and Diehl K 2007 Droplet growth by gravitational coagulation enhanced by turbulence: comparison of theory and measurements *J. Geophys. Res.* **112** D07204
- Rogers R R and Yau M K 1989 *A Short Course in Cloud Physics* (Oxford: Pergamon)
- Sachs D, Lovejoy S and Schertzer D 2002 The Multifractal scaling of cloud radiances from IM to IKM *Fractals* **10** 253–64
- Salazar J P L C, de Jong J, Cao L, Woodward S, Meng H and Collins L R 2008 Experimental and numerical investigation of inertial particle clustering in isotropic turbulence *J. Fluid Mech.* **600** 245–56
- Sato Y and Yamamoto K 1987 Lagrangian measurement of fluid-particle motion in an isotropic turbulent field *J. Fluid Mech.* **175** 183–99
- Saw E W, Shaw R A, Ayyalasomayajula S, Chuang P K and Gylfason A 2008 Inertial clustering of particles in high Reynolds-number turbulence *Phys. Rev. Lett.* **100** 214501
- Sawford B L 1991 Reynolds-numbers effects in Lagrangian stochastic-models of turbulent dispersion *Phys. Fluids A* **3** 1577–86
- Shaw R A 2003 Particle-turbulence interactions in atmospheric clouds *Annu. Rev. Fluid Mech.* **35** 183–227
- Shaw R A, Kostinski A B and Larsen M L 2002 Towards quantifying droplet clustering in clouds *Q. J. R. Meteorol. Soc.* **128** 1043–57
- Shaw R A, Reade W C and Collins L R 1998a Preferential concentration of cloud droplets by turbulence: effects on the early evolution of cumulus cloud droplet spectra *J. Atmos. Sci.* **55** 1965–76
- Shaw R A, Reade W C, Collins L R and Verlinde J 1998b Preferential concentration of cloud droplets by turbulence: effects on the early evolution of cumulus cloud droplet spectra *J. Atmos. Sci.* **55** 1965–76
- Shaw R A and Oncley S P 2001 Acceleration intermittency and enhanced collision kernels in turbulent clouds *Atmos. Res.* **59–60** 77–87
- Shields C 2004 *Constable's Skies 2004* ed F Bancroft (New York: Salander-O'Reilly Galleries) pp 111–23
- Snyder W H and Lumley J L 1971 Some measurements of particle velocity autocorrelation functions in a turbulent flow *J. Fluid Mech.* **48** 41
- Squires K D and Eaton J K 1991 Preferential concentration of particles by turbulence *Phys. Fluids A* **3** 1169–78
- Sundaram S and Collins L R 1997 Collision statistics in an isotropic particle-laden turbulent suspension. Part 1. Direct numerical simulations. *J. Fluid Mech.* **335** 75–109
- Tennekes H and Lumley J L 1972 *A First Course in Turbulence* (Cambridge, MA: MIT Press)
- Uhlig E M, Borrmann S and Jaenicke R 1998 Holographic *in-situ* measurements of the spatial droplet distribution in stratiform clouds *Tellus B* **50** 377–87
- Vaillancort P A and Yau M K 2000 Review of particle-turbulence interactions and consequences for cloud physics *Bull. Am. Meteorol. Soc.* **81** 285–98
- Vedula P and Yeung P K 1999 Similarity scaling of acceleration and pressure statistics in numerical simulations of isotropic turbulence *Phys. Fluids* **11** 1208–20
- Voth G A, La Porta A, Crawford A M, Alexander J and Bodenschatz E 2002 Measurement of particle accelerations in fully developed turbulence *J. Fluid Mech.* **469** 121
- Vohl O, Mitra S K, Wurzler S C and Pruppacher H R 1999 A wind tunnel study of the effects of turbulence on the growth of cloud drops by collision and coalescence *J. Atmos. Sci.* **56** 4088–99
- Warhaft Z 2000 Passive scalars in turbulent flows *Annu. Rev. Fluid Mech.* **32** 303–40
- Warhaft Z 2002 Turbulence in nature and in the laboratory *Proc. Natl. Acad. Sci. USA* **99** (Suppl. 1) 2481–86
- Wells M R and Stock D E 1983 The effect of crossing trajectories on the dissipation of particles in a turbulent flow *J. Fluid Mech.* **136** 31–62
- Wilson C T R 1911 On a method of making visible the paths of ionizing particles through gas *Proc. R. Soc. A* **85** 285–88
- Wilson C T R 1954 Ben Nevis sixty years ago *Weather* **9** 309–11
- Wilson C T R 1965 *Noble Lectures, Physics 1922–1941* (Amsterdam: Elsevier)
- Wood A M, Hwang W and Eaton J K 2005 Preferential concentration of particles in homogeneous and isotropic turbulence *Int. J. Multiph. Flow* **31** 1220–30
- Xu H and Bodenschatz E 2008 Motion of inertial particles with size larger than the Kolmogorov scale in turbulent flows *Physica D* doi: 10.1016/j.physd.2008.04.022
- Yaglom A M 1949 On the acceleration field in a turbulent flow *C.R. Akad. USSR* **67** 795–8
- Yoshimoto H and Goto S 2007 Self-similar clustering of inertial particles in homogeneous turbulence *J. Fluid Mech.* **577** 275–86
- Zerefos C S *et al* 2007 Atmospheric effects of volcanic eruptions as seen by famous artists and depicted in their paintings *Atmos. Chem. Phys.* **7** 4027–42